KSTLE International Journal, Vol. 10, No. 1/2, December 2009, pp. 6-12

The Effect of Oil Supply Conditions on the Dynamic Performance of a Hydrodynamic Journal Bearing

Sang-Ik Son and Kyung-Woong Kim†

School of Mechanical, Aerospace & Systems Engineering, Korea Advanced Institute of Science and Technology, Daejeon, Korea

(Received 1 September 2009; Revised 31 October 2009)

Abstract: In this study, the effect of oil supply conditions on the dynamic performance of a hydrodynamic journal bearing is analyzed numerically. Axial length, circumferential length and location of oil grooves are considered as oil supply conditions. The perturbation equations of the perturbed film contents are obtained by applying Elrod's universal equation implementing JFO film rupture / reformation boundary conditions to Lund's infinitesimal perturbation method. The dynamic coefficients of a hydrodynamic journal bearing are calculated by solving the perturbation equations, and the linear stability analysis is carried out by using those for a variety of oil supply conditions.

Keywords: *Hydrodynamic journal bearing, oil supply condition, cavitation, linear stability*

Nomenclature

C_{ij}	Dimensionless damping coefficient
F_X, F_Z	Dimensionless reaction force components in X and Z direction
H	Dimensionless film thickness
K_{ij}	Dimensionless stiffness coefficient
M	Dimensionless mass of a journal
M_C	Dimensionless critical mass
P	Dimensionless pressure
P_C	Dimensionless cavitation pressure
P_S	Dimensionless oil supply pressure
T	Dimensionless time
W	Dimensionless load
c	Bearing clearance
c_{ij}	Damping coefficient
d	Bearing diameter
f_x, f_z	Reaction force components in x and z direction
g_s	Switch function
h	Film thickness
k_{ij}	Stiffness coefficient
l	Bearing width
l_g	Axial length of oil grooves
n	Normal direction to interfaces between the cavitation region and full film region
p	Pressure
p_c	Cavitation pressure
r	Bearing radius
w	Load
B	Dimensionless bulk modulus
Ω	Whirl ratio
Ω_C	Critical whirl ratio
β	Bulk modulus
γ	Oil groove angle
η	Oil viscosity
θ_{g1}, θ_{g2}	Location of oil groove$_{\#1}$ and groove$_{\#2}$
θ_f	Film content
$(\theta_f)_i$	Perturbed film content
ρ	Mixture density of both oil and air
ρ_c	Oil density at the cavitation pressure
ω	Rotating speed of a journal
ω_w	Whirl speed of a journal

Subscripts

$_{cavity}$	Cavitation region
$_{full\ film}$	Full film region
$_o$	Equilibrium position
$_{Oil\ groove}$	Oil groove

1. Introduction

Lubricating oil needs to be supplied sufficiently through oil grooves in order for a hydrodynamic journal bearing to operate

†Corresponding author; taeho@kaist.ac.kr
Tel: +82-42-350-3215, Fax : +82-42-350-3210

properly. The performance of a hydrodynamic journal bearing varies with oil supply conditions such as the location and specification of oil grooves. Therefore, when designing a hydrodynamic journal bearing, it is essential to analyze the effect of oil supply conditions on the performance of a hydrodynamic journal bearing.

Many studies have been carried out to analyze the effect of oil supply conditions on the performance of a hydrodynamic journal bearing. Ken et al. [1] analyzed the effect of oil supply pressure and the location of axial grooves on the static performance of a hydrodynamic journal bearing. So et al. [2] analyzed the cooling effect of lubricating oil by varying oil supply pressure and the length of axial grooves of a hydrodynamic journal bearing. They reported that the cooling effect of lubricating oil and load capacity decreased as oil supply pressure and the length of axial grooves decreased.

In the above studies, however, the cavitation region where cavitation occurred was not predicted appropriately because the position of the maximum film thickness was considered as the film reformation position, where violated the principle of mass conservation. It is essential to predict the cavitation region appropriately because the cavitation region varies with oil supply conditions and affects the performance of a hydrodynamic journal bearing greatly.

Many efforts have been made to predict the cavitation region appropriately when analyzing the performance of a hydrodynamic journal bearing. Zhang [3] calculated the dynamic coefficients of an infinitely wide journal bearing and carried out the linear stability analysis by varying oil supply pressure and the location of an axial groove. Jeong et al. [4] analyzed the effect of the location of axial, spiral and X-shaped grooves on the static performance of a hydrodynamic journal bearing. Vijayaraghavan et al. [5] analyzed the static performance of a hydrodynamic journal bearing by varying the number and location of axial and cylindrical grooves. They reported that the cavitation region varied with the location of oil grooves and load capacity became the greatest when oil grooves were located in the cavitation region or the position of the maximum film thickness. Costa et al. [6] analyzed the effect of oil supply pressure, oil temperature, the location and specification of oil grooves on the static performance of a hydrodynamic journal bearing and compared analysis results with experiments. Wang et al. [7, 8] analyzed the static and dynamic performance of an infinitely wide journal bearing by varying oil supply pressure and the location of an oil groove.

Most of previous studies focused on analyzing the effect of oil supply conditions on the static performance of a hydrodynamic journal bearing, so it was insufficient to analyze that on the dynamic performance of a hydrodynamic journal bearing.

In this study, axial, circumferential length and location of oil grooves are considered as oil supply conditions and the effect of those on the dynamic performance of a hydrodynamic journal bearing is analyzed numerically. Elrod's universal equation which implements JFO film rupture / reformation boundary conditions is adopte in order to consider the effect of the cavitation region. The perturbation equations are obtained by applying Elrod's universal equation to Lund's infinitesimal perturbation method, and the linear stability analysis of a hydrodynamic journal bearing is carried out by solving those for oil supply conditions.

2. Analysis

2.1. Governing equation

The pressure distribution of fluid film in a hydrodynamic journal bearing is determined by Reynolds equation.

$$\frac{1}{r^2}\frac{\partial}{\partial\theta}\left(\frac{\rho h^3}{12\eta}\frac{\partial p}{\partial\theta}\right)+\frac{\partial}{\partial y}\left(\frac{\rho h^3}{12\eta}\frac{\partial p}{\partial y}\right)=\frac{\omega}{2}\frac{\partial}{\partial\theta}(\rho h)+\frac{\partial}{\partial t}(\rho h) \quad (1)$$

The clearance of a hydrodynamic journal bearing has converging-diverging geometry. Cavitation occurs when the pressure of fluid film drops below the saturation pressure within the clearance having diverging geometry. The cavitation region can be predicted by finding the film rupture and reformation positions. Jakobsson, Floberg [9] and Olsson [10] formulated JFO boundary conditions based on the principle of mass conservation at the interfaces between the cavitation region and full film region. JFO boundary conditions are expressed as

$$\frac{\partial p}{\partial n}=0, p=p_c \quad (2)$$

$$\left(\frac{h^2}{12\eta}\right)\left(\frac{\partial p}{\partial n}\right)_{full\ fulm}=\frac{u_n}{2}[1-(\theta_f)_{cavity}], p=p_c \quad (3)$$

where the cavitation pressure, p_c represents the pressure of fluid film in the cavitation region, and film content, θ_f represents the ratio of the mixture density of both oil and air, ρ to oil density at the cavitation pressure, ρ_c. Equation (2) is the boundary condition at the film rupture position, and Eq. (3) is that at the film reformation position.

Elrod and Adams [11] proposed Elrod's universal equation satisfying JFO boundary conditions.

$$\frac{1}{r^2}\frac{\partial}{\partial\theta}\left(\frac{\beta g_s h^3}{12\eta}\frac{\partial\theta_f}{\partial\theta}\right)+\frac{\partial}{\partial y}\left(\frac{\beta g_s h^3}{12\eta}\frac{\partial\theta_f}{\partial y}\right)$$
$$=\frac{\omega}{2}\frac{\partial}{\partial\theta}(\theta_f h)+\frac{\partial}{\partial t}(\theta_f h) \quad (4)$$

Film content is related with the pressure of fluid film by the expression as

$$p=p_c+g_s\beta ln\theta_f \quad (5)$$

where

$$g_s=\begin{cases}1 \text{ in the full film region } (\theta_f\geq 1)\\ 0 \text{ in the cavitation region } (\theta_f<1)\end{cases} \quad (6)$$

$$\beta=\rho\frac{\partial p}{\partial\rho} \quad (7)$$

In the above equations, switch function, g_s is a variable to divide into the cavitation region and full film region, and fluid bulk modulus, β represents the reciprocal of fluid compressibility defining how much fluid can be compressed.

Dimensionless forms of Eq. (4) and (5) are expressed as

$$\frac{\partial}{\partial\theta}\left(\frac{BH^3 g_s}{12}\frac{\partial\theta_f}{\partial\theta}\right)+\left(\frac{r}{l}\right)^2\frac{\partial}{\partial Y}\left(\frac{BH^3 g_s}{12}\frac{\partial\theta_f}{\partial Y}\right) = \frac{1}{2}\frac{\partial}{\partial\theta}(\theta_f H)+\Omega\frac{\partial}{\partial T}(\theta_f H) \tag{8}$$

$$P = \frac{p}{\eta\omega}\left(\frac{c}{r}\right)^2 = P_C + g_s B\ln\theta_f \tag{9}$$

where

$$Y = \frac{y}{l},\ B = \frac{\beta}{\eta\omega}\left(\frac{c}{r}\right)^2,\ H = \frac{h}{c},\ \Omega = \frac{\omega_w}{\omega},\ T = \omega_w t \tag{10}$$

2.2. Linear stability analysis

The bearing dynamic coefficients are calculated by using Lund's infinitesimal perturbation method, which formulates the perturbation equations from the first-order Taylor expansion of the pressure distribution in fluid film proposed by Lund and Thomsen [12]. Assuming that the amplitude of a journal motion is infinitesimal about the equilibrium position, dimensionless film thickness changed by a journal motion is expressed as

$$H = H_0 + \sin\theta\Delta X + \cos\theta\Delta Z \tag{11}$$

where

$$X = \frac{x}{c},\ Z = \frac{z}{c} \tag{12}$$

In Eq. (11), H_0 represents dimensionless film thickness at the equilibrium position.

Film content changed by a journal motion is expressed as

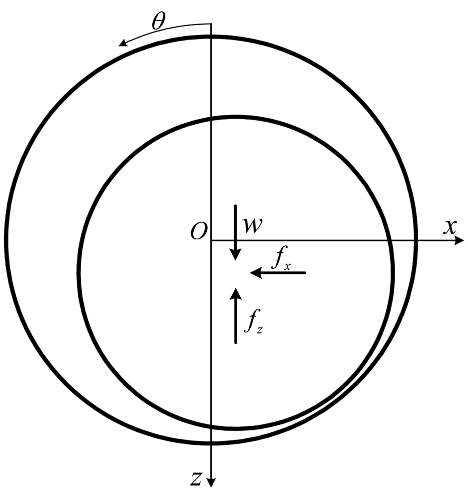

Fig. 1. Force components acting on a journal.

$$\theta_f = (\theta_f)_0 + \frac{\partial\theta_f}{\partial X}\Delta X + \frac{\partial\theta_f}{\partial Z}\Delta Z + \frac{\partial\theta_f}{\partial\dot{X}}\Delta\dot{X} + \frac{\partial\theta_f}{\partial\dot{Z}}\Delta\dot{Z} = (\theta_f)_0 + (\theta_f)_X\Delta X + (\theta_f)_z\Delta Z + (\theta_f)_{\dot{X}}\Delta\dot{X} + (\theta_f)_{\dot{Z}}\Delta\dot{Z} \tag{13}$$

where

$$\dot{X} = \frac{dX}{dT} = \frac{1}{c\omega_w}\frac{dx}{dt},\ \dot{Z} = \frac{dZ}{dT} = \frac{1}{c\omega_w}\frac{dz}{dt} \tag{14}$$

In Eq. (13), $(\theta_f)_0$ represents the film content at the equilibrium position, and other terms represent perturbed film contents. It is assumed that the cavitation region at the equilibrium position is not changed by the infinitesimal amplitude of a journal motion and the film content of couette and unsteady terms of Eq. (8) is unity in the full film region because fluid density in the full film region is nearly close to that at the cavitation pressure. In the full film region, then, Eq. (8) is expressed as

$$\frac{\partial}{\partial\theta}\left(\frac{BH^3}{12}\frac{\partial\theta_f}{\partial\theta}\right)+\left(\frac{r}{l}\right)^2\frac{\partial}{\partial Y}\left(\frac{BH^3}{12}\frac{\partial\theta_f}{\partial Y}\right) = \frac{1}{2}\frac{\partial H}{\partial\theta}+\Omega\frac{\partial H}{\partial T} \tag{15}$$

Substituting Eq. (11) and (13) into Eq. (15) and retaining only the first-order terms, five perturbation equations are obtained as

$$\frac{\partial}{\partial\theta}\left\{\frac{BH_0^3}{12}\frac{\partial}{\partial\theta}(\theta_f)_0\right\}+\left(\frac{r}{l}\right)^2\frac{\partial}{\partial Y}\left\{\frac{BH_0^3}{12}\frac{\partial}{\partial Y}(\theta_f)_0\right\} = \frac{1}{2}\frac{\partial H_0}{\partial\theta} \tag{16}$$

$$\frac{\partial}{\partial\theta}\left\{\frac{BH_0^3}{12}\frac{\partial}{\partial\theta}(\theta_f)_{\dot{X}}\right\}+\left(\frac{r}{l}\right)^2\frac{\partial}{\partial Y}\left\{\frac{BH_0^3}{12}\frac{\partial}{\partial Y}(\theta_f)_{\dot{X}}\right\} = \Omega\sin\theta \tag{17}$$

$$\frac{\partial}{\partial\theta}\left\{\frac{BH_0^3}{12}\frac{\partial}{\partial\theta}(\theta_f)_{\dot{Z}}\right\}+\left(\frac{r}{l}\right)^2\frac{\partial}{\partial Y}\left\{\frac{BH_0^3}{12}\frac{\partial}{\partial Y}(\theta_f)_{\dot{Z}}\right\} = \Omega\cos\theta \tag{18}$$

$$\frac{\partial}{\partial\theta}\left\{\frac{BH_0^3}{12}\frac{\partial}{\partial\theta}(\theta_f)_X\right\}+\left(\frac{r}{l}\right)^2\frac{\partial}{\partial Y}\left\{\frac{BH_0^3}{12}\frac{\partial}{\partial Y}(\theta_f)_X\right\} = \frac{1}{2}\cos\theta - \frac{BH_0^3}{4}\left\{\frac{\partial}{\partial\theta}(\theta_f)_0\right\}\left\{\frac{\partial}{\partial\theta}\left(\frac{\sin\theta}{H_0}\right)\right\} - \frac{3\sin\theta}{2H_0}\frac{\partial H_0}{\partial\theta} - \left(\frac{r}{l}\right)^2\frac{BH_0^3}{4}\left\{\frac{\partial}{\partial Y}(\theta_f)_0\right\}\left\{\frac{\partial}{\partial Y}\left(\frac{\sin\theta}{H_0}\right)\right\} \tag{19}$$

$$\frac{\partial}{\partial\theta}\left\{\frac{BH_0^3}{12}\frac{\partial}{\partial\theta}(\theta_f)_Z\right\}+\left(\frac{r}{l}\right)^2\frac{\partial}{\partial Y}\left\{\frac{BH_0^3}{12}\frac{\partial}{\partial Y}(\theta_f)_Z\right\} = -\frac{1}{2}\sin\theta - \frac{BH_0^3}{4}\left\{\frac{\partial}{\partial\theta}(\theta_f)_0\right\}\left\{\frac{\partial}{\partial\theta}\left(\frac{\cos\theta}{H_0}\right)\right\} - \frac{3\cos\theta}{2H_0}\frac{\partial H_0}{\partial\theta} - \left(\frac{r}{l}\right)^2\frac{BH_0^3}{4}\left\{\frac{\partial}{\partial Y}(\theta_f)_0\right\}\left\{\frac{\partial}{\partial Y}\left(\frac{\cos\theta}{H_0}\right)\right\} \tag{20}$$

Equation (16) is identical to Elrod's universal equation in the full film region under steady state. The solution of Eq. (16) is obtained by using Elrod's cavitation algorithm [13]. Equations (17)~(20) are solved by using the finite difference method with Gauss-Seidel iteration. The boundary conditions for calculating perturbed film contents are

$$(\theta_f)_\lambda\big|_{cavity} = (\theta_f)_\lambda\big|_{Y=0} = (\theta_f)_\lambda\big|_{Y=1} = (\theta_f)_\lambda\big|_{oil\ groove} = 0 \quad (21)$$

$$\lambda = X, Z, \dot{X}, \dot{Z}$$

Figure 1 shows a static load, w and reaction force components, f_x and f_z. Dimensionless reaction forces changed by the infinitesimal amplitude of a journal motion are expressed as

$$\begin{Bmatrix} F_X \\ F_Z \end{Bmatrix} = \begin{Bmatrix} (F_X)_0 \\ (F_Z)_0 \end{Bmatrix} + [K]\begin{Bmatrix} \Delta X \\ \Delta Z \end{Bmatrix} + [C]\begin{Bmatrix} \Delta\dot{X} \\ \Delta\dot{Z} \end{Bmatrix} \quad (22)$$

where

$$\begin{Bmatrix} (F_X)_0 \\ (F_Z)_0 \end{Bmatrix} = \frac{1}{\eta\omega r l}\left(\frac{c}{r}\right)^2 \begin{Bmatrix} (f_x)_0 \\ (f_z)_0 \end{Bmatrix} = \int_0^1\int_0^{2\pi}[P_C + g_s B\{(\theta_f)_0 - 1\}]\begin{Bmatrix} -\sin\theta \\ -\cos\theta \end{Bmatrix} d\theta dY \quad (23)$$

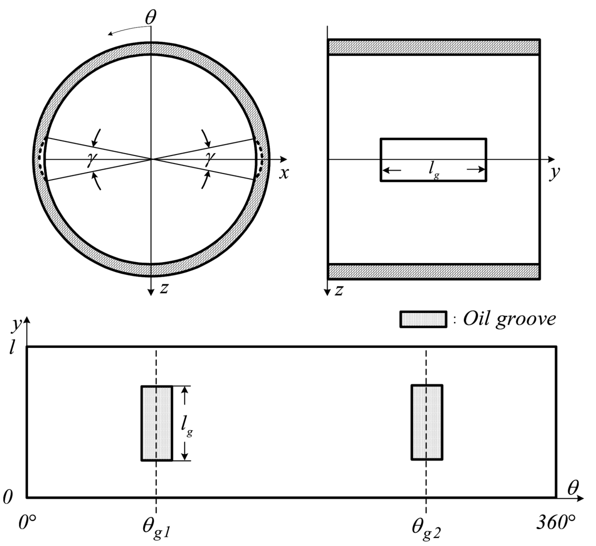

Fig. 2. Axial type grooved journal bearing.

Table 1. Specification of parameter values

Bearing width / bearing diameter (l / d)	1.0
Bearing clearance / bearing diameter (c / d)	1/1000
Axial length of oil grooves / bearing width (l_g / l)	1/2
Oil groove angle (γ)	20°
Location of oil groove$_{\#1}$ (θ_{g1})	90°
Location of oil groove$_{\#2}$ (θ_{g2})	270°
Dimensionless fluid bulk modulus (B)	300
Dimensionless oil supply pressure (P_S)	0.0
Dimensionless cavitation pressure (P_C)	0.0

$$[K] = \begin{bmatrix} K_{XX} & K_{XZ} \\ K_{ZX} & K_{ZZ} \end{bmatrix} = \frac{1}{\eta\omega l}\left(\frac{c}{r}\right)^3\begin{bmatrix} k_{xx} & k_{xz} \\ k_{zx} & k_{zz} \end{bmatrix} = \int_0^1\int_0^{2\pi} g_s B\begin{Bmatrix} -\sin\theta \\ -\cos\theta \end{Bmatrix}\{(\theta_f)_X (\theta_f)_Z\} d\theta dY \quad (24)$$

$$[C] = \begin{bmatrix} C_{XX} & C_{XZ} \\ C_{ZX} & C_{ZZ} \end{bmatrix} = \frac{1}{\eta l}\left(\frac{c}{r}\right)^3\begin{bmatrix} c_{xx} & c_{xz} \\ c_{zx} & c_{zz} \end{bmatrix} = \int_0^1\int_0^{2\pi} g_s \frac{B}{\Omega}\begin{Bmatrix} -\sin\theta \\ -\cos\theta \end{Bmatrix}\{(\theta_f)_{\dot{X}}(\theta_f)_{\dot{Z}}\} d\theta dY \quad (25)$$

In the above equations, the terms indicated by subscript *0* represent dimensionless reaction forces at equilibrium position and [*K*] and [*C*] represent dimensionless stiffness and damping matrix.
Dimensionless load is expressed as

$$W = \frac{w}{\eta\omega r l}\left(\frac{c}{r}\right)^2 = \sqrt{(F_X)_0^2 + (F_Z)_0^2} \quad (26)$$

Assuming that a journal and bearing are rigid and a journal has only translational motion, the dimensionless equation of a journal motion is expressed as

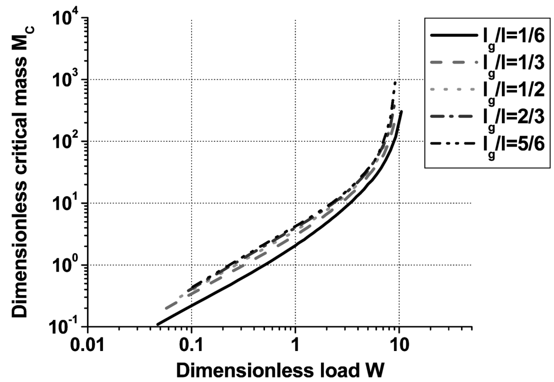

(a) M_C vs. W

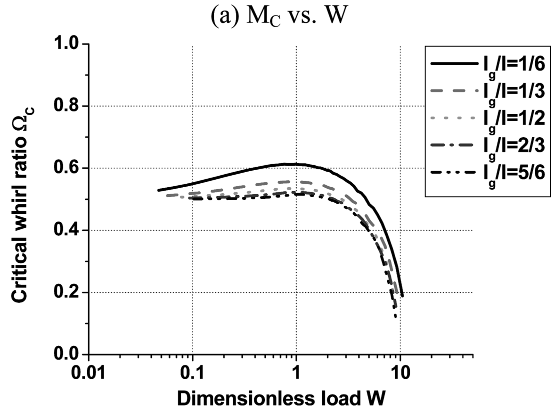

(b) Ω_C vs. W

Fig. 3. The linear stability analysis of a journal bearing with variation of axial length of oil grooves.

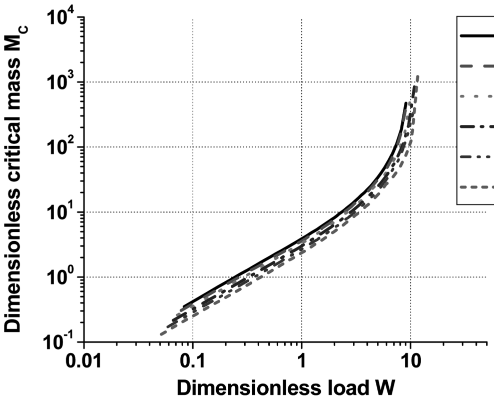

(a) M_C vs. W

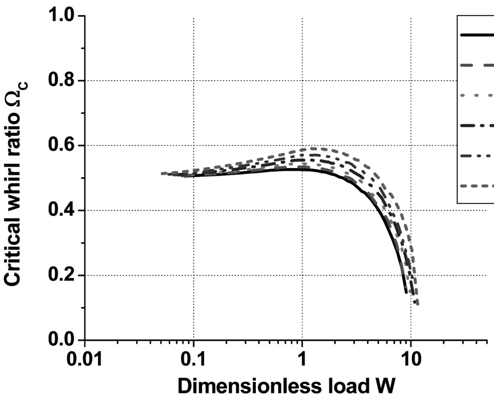

(b) Ω_C vs. W

Fig. 4. The linear stability analysis of a journal bearing with variation of circumferential length of oil grooves.

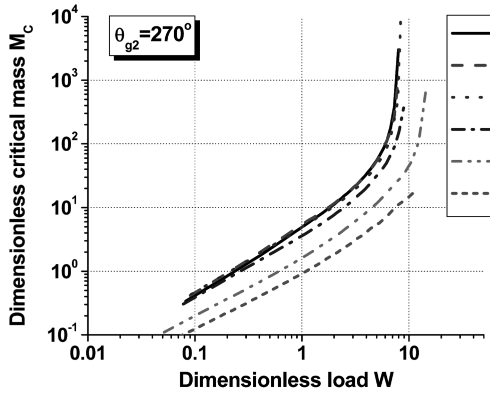

(a) M_C vs. W

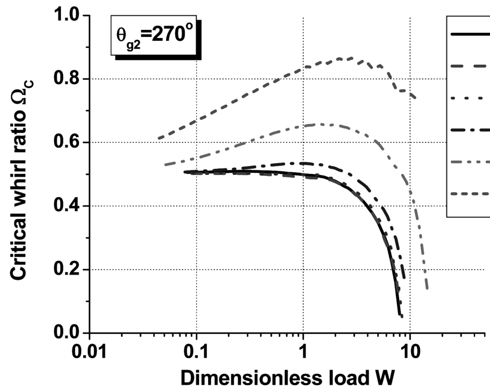

(b) Ω_C vs. W

Fig. 5. The linear stability analysis of a journal bearing with variation of oil groove$_{\#1}$ location.

$$\begin{bmatrix} \Omega^2 M & 0 \\ 0 & \Omega^2 M \end{bmatrix} \begin{Bmatrix} \ddot{X} \\ \ddot{Z} \end{Bmatrix} + \begin{bmatrix} \Omega C_{XX} & \Omega C_{XZ} \\ \Omega C_{ZX} & \Omega C_{ZZ} \end{bmatrix} \begin{Bmatrix} \dot{X} \\ \dot{Z} \end{Bmatrix} + \begin{bmatrix} K_{XX} & K_{XZ} \\ K_{ZX} & K_{ZZ} \end{bmatrix} \begin{Bmatrix} X \\ Z \end{Bmatrix} = \begin{Bmatrix} 0 \\ 0 \end{Bmatrix} \tag{27}$$

where

$$M = \frac{m\omega}{\eta l}\left(\frac{c}{r}\right)^3, \ddot{X} = \frac{1}{c\omega_w^2}\frac{d^2x}{dt^2}, \ddot{Z} = \frac{1}{c\omega_w^2}\frac{d^2z}{dt^2} \tag{28}$$

When the motion of a journal is stable orbitally, it is expressed as

$$\begin{Bmatrix} X \\ Z \end{Bmatrix} = \begin{Bmatrix} X_0 \\ Z_0 \end{Bmatrix} e^{iT} \tag{29}$$

Substituting Eq. (29) into Eq. (27), the dimensionless equation of a journal motion is expressed as

$$\begin{bmatrix} -\Omega^2 M + i\Omega C_{XX} + K_{XX} & i\Omega C_{XZ} + K_{XZ} \\ i\Omega C_{ZX} + K_{ZX} & -\Omega^2 M + i\Omega C_{ZZ} + K_{ZZ} \end{bmatrix} \begin{Bmatrix} X_0 \\ Z_0 \end{Bmatrix} = \begin{Bmatrix} 0 \\ 0 \end{Bmatrix} \tag{30}$$

The determinant should be zero for a nontrivial solution of Eq. (30). Dimensionless mass of a journal, M and whirl ratio, Ω satisfying the determinant is zero are dimensionless critical mass, M_C and critical whirl ratio, Ω_C.

2.3. Test bearing

Figure 2 shows the geometry of a hydrodynamic journal bearing with two axial grooves and Table 1 represents its parameter values. A journal rotates in a counterclockwise direction and dimensionless pressure at the both end sides of a bearing is equal to zero.

The analysis is carried out by varying one parameter among oil supply conditions and keeping the others constant in order to analyze the effect of each parameter on the dynamic performance of a hydrodynamic journal bearing.

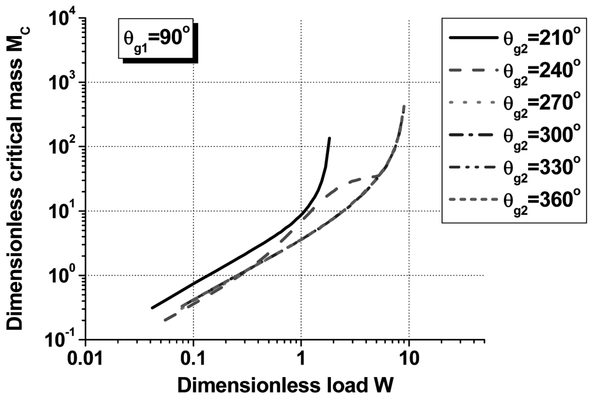

(a) M_C vs. W

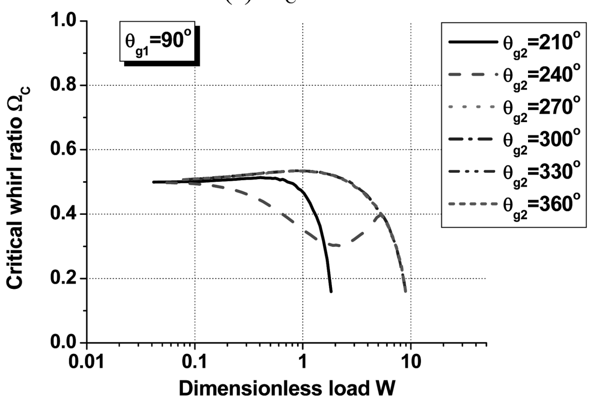

(b) Ω_C vs. W

Fig. 6. The linear stability analysis of a journal bearing with variation of oil groove$_{\#2}$ location.

3. Results and Discussion

3.1. The effect of the axial length of oil grooves

The effect of axial length of oil grooves on the dynamic performance of a hydrodynamic journal bearing is analyzed by increasing the ratio of axial length of oil grooves, l_g to bearing width, l from 1/6 to 5/6.

Figure 3 represents plots of dimensionless critical mass and critical whirl ratio with respect to dimensionless load. As shown in Fig. 3 (a), dimensionless critical mass increases with the increase in dimensionless load for the given ratio of axial length of oil grooves to bearing width. When dimensionless mass of a journal is greater than dimensionless critical mass, whirl instability occurs. Therefore, dimensionless mass of a journal should be lower than dimensionless critical mass in order for a rotor-bearing system to operate stably without whirl instability. Dimensionless critical mass increases abruptly as dimensionless load is nearly close to ten. When dimensionless load exceeds that, a rotor-bearing system is always stable regardless of dimensionless mass of a journal. This tendency can also be observed in analysis results of the circumferential length and location of oil grooves. For the dimensionless load given, dimensionless critical mass increases with the increase in the ratio of axial length of oil grooves to bearing width. That means the stability of a rotor-bearing system increases with the increase in axial length of oil grooves. As shown in Fig. 3 (b), critical whirl ratio decreases with the increase in the ratio of axial length of oil grooves to bearing width for the dimensionless load given.

3.2. The effect of the circumferential length of oil grooves

The effect of circumferential length of oil grooves on the dynamic performance of a hydrodynamic journal bearing is analyzed by increasing oil groove angle, γ from 10° to 60°. The circumferential length of oil grooves increases with the increase in oil groove angle.

Figure 4 represents plots of dimensionless critical mass and critical whirl ratio with respect to dimensionless load. As shown in Fig. 4 (a), dimensionless critical mass decreases with the increase in oil groove angle for the dimensionless load given. Therefore, the circumferential length of oil grooves should be shorter in order to improve the stability of a rotor-bearing system. As shown in Fig. 4 (b), critical whirl ratio increases with the increase in oil groove angle for the dimensionless load given.

3.3. The effect of the location of oil grooves

The effect of location of oil grooves on the dynamic performance of a hydrodynamic journal bearing is analyzed by varying the location of oil groove$_{\#1}$, θ_{g1} and oil groove$_{\#2}$, θ_{g2}.

Figure 5 represents plots of dimensionless critical mass and critical whirl ratio with respect to dimensionless load by varying the location of oil groove$_{\#1}$ from 0° to 150° and keeping the location of oil groove$_{\#2}$ 270°. As shown in Fig. 5 (a), the location of oil groove$_{\#1}$ where dimensionless critical mass becomes the greatest varies with dimensionless load. Dimensionless critical mass is greater when oil groove$_{\#1}$ is located between 0° and 60° than between 60° and 150° for the dimensionless load given and decreases as the location of oil groove$_{\#1}$ increases from 60° to 150°. Therefore, oil groove$_{\#1}$ should be located between 0° and 60° in order to improve the stability of a rotor-bearing system. As shown in Fig. 5 (b), critical whirl ratio increases with the increase in location of oil groove$_{\#1}$ for the dimensionless load given.

Figure 6 represents plots of dimensionless critical mass and critical whirl ratio with respect to dimensionless load by varying the location of oil groove$_{\#2}$ from 210° to 360° and keeping the location of oil groove$_{\#1}$ 90°. As shown in Fig. 6 (a), dimensionless critical mass becomes the greatest when oil groove$_{\#2}$ is located at 210° for the dimensionless load given. Therefore, oil groove$_{\#2}$ should be located near 210° in order to improve the stability of a rotor-bearing system. As shown in Fig. 6 (b), critical whirl ratio is smaller when oil groove$_{\#2}$ is located at 210° or 240° than at the others for the dimensionless load given.

4. Conclusion

In this study, the effect of oil supply conditions on the dynamic performance of a hydrodynamic journal bearing has been analyzed numerically. Elrod's universal equation was used in order to predict the cavitation region varying with oil supply conditions accurately. The conclusions are as follows:

1. Dimensionless critical mass increases as the axial length of oil grooves increases or the circumferential length of oil grooves decreases.
2. Dimensionless critical mass is greater when oil groove$_{\#1}$ is located between 0^o and 60^o than between 60^o and 150^o, and the location of oil groove$_{\#1}$ where dimensionless critical mass becomes the greatest varies with dimensionless load.
3. Dimensionless critical mass becomes the greatest when oil groove$_{\#2}$ is located at 210^o.

Acknowledgment

This work was supported by the Brain Korea 21 Project.

References

1. Ken, I., Mori, H., An Analysis of Lubricating Film Journal Bearing-Effect of oil Supply Condition on the Static Performance, JSLE, No. 4, 1984.
2. So, H., Shieh, J. A., The Cooling Effects of Supply Oil on Journal Bearings for Varying Inlet Conditions, Tribology International, Vol. 20, pp.79-89, 1987.
3. Zhang, Y., Dynamic Properties of flexible Journal Bearings of Infinite Width Considering Oil Supply Condition and Pressure, Wear, Vol. 130, pp. 53-68, 1989.
4. Jeong, K. M., Kim, K. W., The Effects of Oil Supply Conditions on the Static Characteristics of Plain Journal Bearings, J. of the KSTLE, Vol. 6, No. 2, pp. 76-87, 1990.
5. Vijayaraghavan, D., Keith JR., T. G., Effect of Type and Location of Oil Groove on the Performance of Journal Bearings, Tribology Transactions, Vol. 35, pp. 98-106, 1992.
6. Costa, L., Miranda, A. S., Fillon, M., Claro, J. C. P., An Analysis of the Influence of Oil Supply Conditions on the Thermohydrodynamic Performance of a Single-Groove Journal Bearing, Proc Instit Mech Eng Part J: J Eng Tribology, Vol. 217, pp. 133-144, 2003.
7. Wang, J. K., Khonsari, M. M., Effects of Oil Inlet Pressure and Inlet Position of Axially Grooved Infinitely Long Journal Bearings. Part I: Analytical Solutions and Static Performance, Tribology International, Vol. 41, pp. 119-131, 2008.
8. Wang, J. K., Khonsari, M. M., Effects of Oil Inlet Pressure and Inlet Position of Axially Grooved Infinitely Long Journal Bearings. Part II: Nonlinear Instability Analysis, Tribology International, Vol. 41, pp. 132-140, 2008.
9. Floberg, L., Jakobsson, B., The Finite Journal Bearing Considering Vaporization, Transactions Chalmers Univ. Technology, Goteborg, 1957.
10. Olsson, K., Cavitation in Dynamically Loaded Bearings, Transactions Chalmers Univ. Technology, Goteborg, 1965.
11. Elrod, H. G., Adams, M. L., A Computer Program for Cavitation and Starvation Problems, Cavitation and Related Phenomena in Lubrication, Proceedings of the 1st Leeds-Lyon Symposium on Tribology, Leeds Univ., pp. 37-41, 1974.
12. Lund, J. W., Thomsen, K. K., Calculation Method and Data for the Dynamic Coefficients of Oil-Lubricated Journal Bearings, Proc. of the ASME, Minneapolis, pp. 1, 1978.
13. Elrod, H. G., A Cavitation Algorithm, ASME J. of Lubrication Technology, Vol. 103, pp. 350-354, 1981.